Measurement of Isothermal Vapor-Liquid Equilibria for Acetone–*n*-Heptane Mixtures Using Modified Gillespie Still

VENKATACHALAPATI O. MARIPURI and GERALD A. RATCLIFF[1]
Department of Chemical Engineering, McGill University, Montreal, Canada

The Gillespie-type still used by Lu was modified to provide a better approach to equilibrium. It was tested by comparing experimental and literature data for binary mixtures of ethanol–benzene and methanol–water. Isothermal vapor-liquid equilibrium data were then determined for acetone–*n*-heptane mixtures at 65°C. Redlich-Kister constants were evaluated by a weighted least-squares fit and are presented.

Vapor-liquid equilibrium data are useful not only for the design of separation equipment, but also for the study of solution properties of nonideal mixtures. As part of a study of the representation of liquid mixtures by group solution models, modifications were made to a Gillespie-type still, and isothermal vapor-liquid equilibrium data were obtained for acetone–*n*-heptane mixtures at 65°C.

EQUILIBRIUM STILL

The equilibrium still employed is shown in Figure 1. It is a modified form of the Gillespie-type still described by Lu et al. (*13*). The modifications included the use of magnetic stirrers in the sampling cells and the reboiler, a bypass line around the sampling cells, and compensatory heating on the equilibrium chamber and the Cottrell tube. Complete details of the still and its operation are given elsewhere (*8*).

Better mixing in the sampling cells gave a more rapid approach to steady-state operation, and in the reboiler gave a closer approach to equilibrium operation by reducing or eliminating the flashing of volatile material. The existence and seriousness of flashing depend on the relative volatilities of the components involved. When differences in relative volatilities are large, it is difficult to avoid flashing in a recirculation still. The reboiler stirrer also gave more regular nucleation of bubbles and better mixing of liquid and vapor prior to entering the Cottrell tube.

The bypass line was used to isolate the sampling cells after the completion of a run. This eliminated possible contamination of the samples from condensation of nonequilibrium vapor generated at the completion of a run owing to the thermal inertia of the heater.

A compensatory heating tape was wrapped around the insulation. The temperature inside the insulation at about $^3/_4$ in. from the equilibrium chamber was monitored by a copper-constantan thermocouple, and was maintained within 2°C of the boiling point of the mixture under consideration by an on-off controller. This feature was designed to reduce the errors due to condensation.

[1] To whom correspondence should be addressed.

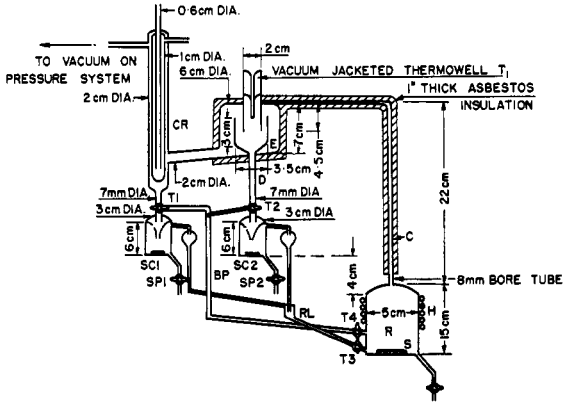

Figure 1. Modified Gillespie still

TEMPERATURE AND PRESSURE MEASUREMENT

A copper-constantan thermocouple calibrated at the ice point and steam point was used to measure the boiling point of the mixture in conjunction with a Leeds-and-Northrup-type K3 potentiometer. The calibration reproduced the data for copper-constantan thermocouples in NBS circular 561 to within 0.02°C, and the tabulated data in the circular were therefore used for direct interpolation. The accuracy of the temperature measurement is believed to be within ±0.05°C. Pressure was measured by a mercury manometer and cathetometer. The pressure was controlled by a Cartesian-type manostat with an accuracy of about 0.2% of the still pressure.

TESTING OF STILL

The still was tested by measuring vapor-liquid equilibria for two test systems at 760 mm Hg and comparing the data with published results. The test systems were binary mix-

Table I. Physical Constants of Ethanol, Methanol, and Benzene

	Refractive index at 25°C		Density at 25°C		Normal bp, °C	
Chemical	Present	Lit. (*10*)	Present	Lit. (*10*)	Present	Lit. (*10*)
Ethanol	1.3594	1.3595–1.3596	0.7850	0.7851	78.2	78.2–78.42
Methanol	1.3287 (at 20°C)	1.3287 (at 20°C)	0.7866	0.7866	64.6	64.5–64.75
Benzene	1.4978	1.4979	0.8735	0.8734	80.1	80.1

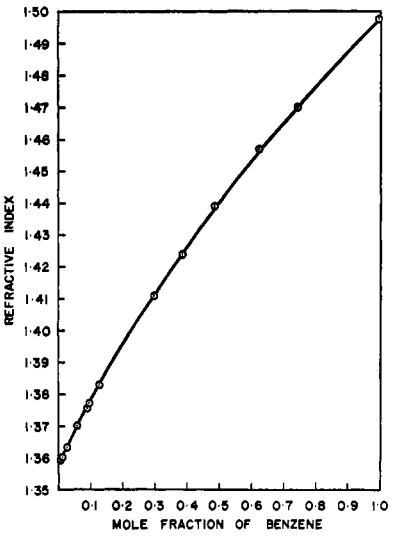

Figure 2. Refractive index–composition data for system ethanol–benzene at 25°C

Table II. Antoine Constants for Ethanol, Methanol, Benzene, and Water

Chemical	A	B	C	Ref.
Ethanol	8.1122	1592.18	226.06	(2)
Methanol[a]	7.9295	1490.19	230.0	(10)
Benzene	6.9128	1214.56	221.16	(4)
Water[a]	7.9172	1666.88	230.0	(10)

[a] Computed from data in ref. 10 using C = 230.0.

tures of ethanol–benzene and methanol–water. Pure absolute alcohol from Gooderham and Worts Ltd, and Baker-analyzed spectrophotometric-grade methyl alcohol were used without further purification. Reagent-grade benzene supplied by Fisher Scientific Co. was redistilled in a packed column with a high reflux ratio, and the fraction boiling between 80.05° and 80.15°C was employed for the study. The packed column had approximately 40 theoretical stages. The properties of the pure compounds are shown in Table I and agree satisfactorily with literature data. Refractive indices were measured using a Carl Zeiss refractometer with a sodium lamp, and densities using a pycnometer. The normal boiling points were measured in the still operating at 760 mm Hg.

Mixture compositions were determined by refractive index (8). A typical calibration plot for the system ethanol–benzene at 25°C is shown in Figure 2. The methanol–water system shows a maximum in refractive index, and the vapor-liquid equilibria in this region were not measured. The vapor pressures of the pure compounds were computed from the Antoine constants shown in Table II. Volumetric data were taken from the literature (1). Second virial coefficients were predicted from Wohl's correlation (12). The activity coefficients were then computed from the classical thermodynamic relation

$$\ln \gamma_i = \ln \frac{\pi y_i}{x_i P_i^0} + \frac{(\beta_i - v_i^L)(\pi - P_i^0)}{RT} \qquad (1)$$

$$i = 1, 2$$

The equation allows for nonideality in the gas phase by using the virial equation truncated to the second term, and also for the effect of pressure on the liquid fugacity.

The experimental equilibrium data are presented in Table III for the two test systems. A comparison of the data with the literature (3, 5, 6, 9, 11) is shown in Figures 3 and 4. The agreement is good.

ACETONE–*n*-HEPTANE SYSTEM

Equilibrium data of this system were determined at 65°C using the still described above. *n*-Heptane supplied by Eastman Organic Chemicals and acetone from Matheson, Coleman and Bell were redistilled, and the fractions with physical properties closely reproducing literature values were employed.

Table III. Experimental Equilibrium Data

(Total pressure = 760 mm Hg)

x_1	y_1	T, K	P_1^0	P_2^0
System Benzene–Ethanol; Component One Is Ethanol				
0.086	0.265	343.9	561.4	566.6
0.112	0.282	342.9	538.4	548.2
0.120	0.308	342.7	533.9	544.6
0.158	0.335	342.2	522.8	535.7
0.200	0.368	341.6	509.7	525.1
0.308	0.410	340.8	493.4	511.8
0.442	0.446	340.8	492.8	511.2
0.604	0.505	341.2	501.2	518.1
0.770	0.590	342.7	534.4	545.0
0.815	0.628	343.5	550.9	558.3
0.841	0.665	344.0	563.7	568.5
0.898	0.744	345.8	607.2	602.8
0.924	0.782	346.9	635.2	624.6
System Methanol–Water; Component One Is Methanol				
0.012	0.114	370.0	2354.3	659.0
0.026	0.157	368.8	2262.1	630.2
0.102	0.430	360.6	1721.9	464.4
0.140	0.514	357.9	1573.2	419.8
0.175	0.560	356.0	1468.3	388.6
0.473	0.765	346.8	1054.7	268.4
0.526	0.794	345.7	1012.6	256.4
0.540	0.801	345.5	1005.0	254.3
0.565	0.805	345.1	990.0	250.1
0.585	0.816	344.6	972.7	245.1
0.662	0.857	343.7	938.3	235.5
0.675	0.865	343.0	915.4	229.1
0.714	0.878	342.2	886.7	221.1
0.850	0.930	340.0	812.9	200.6
0.890	0.956	339.3	791.6	194.7
0.920	0.965	338.8	777.1	190.7

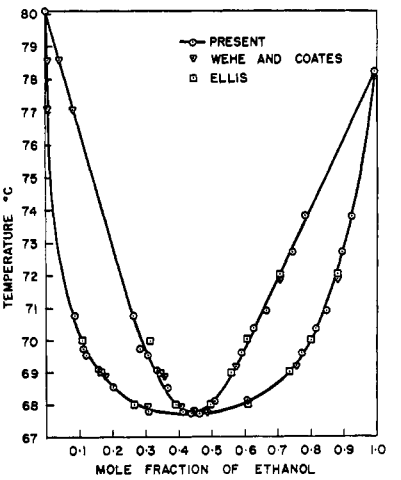

Figure 3. Vapor-liquid equilibrium of ethanol–benzene mixtures at 760 mm Hg

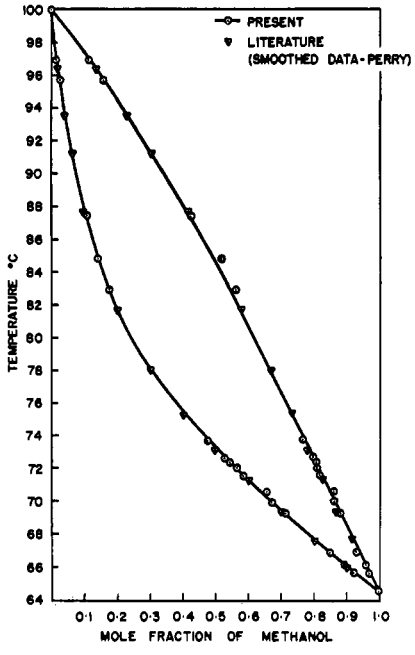

Figure 4. Vapor-liquid equilibrium of methanol–water mixtures at 760 mm Hg

The pure component properties are given in Table IV. Mixture compositions were determined by refractive index measurements. Calibration data are given in ref. *8*.

The activity coefficients were computed from Equation 1, using Wohl's equation for the estimation of second virial coefficients. The experimental values of log (γ_1/γ_2) were fitted by a weighted least-squares method to the three-constant Redlich-Kister equation

$$\log\left(\frac{\gamma_1}{\gamma_2}\right) = B(x_2 - x_1) + C(6\,x_1x_2 - 1) + D(x_2 - x_1)(1 - 8\,x_1x_2) \quad (2)$$

The weighting factors were computed using the method described by Gilmont et al. (*7*). The experimental equilibrium data are given in Table V, and the values of the fitted Redlich-Kister constants are $B = 0.584$, $C = -0.026$, $D = 0.033$. The data are presented graphically in Figures 5 and 6.

Table IV. Physical Properties of Acetone and *n*-Heptane at 25°C

Compound	Refractive index Present	Refractive index Lit.	Density Present	Density Lit.	Normal bp, °C Present	Normal bp, °C Lit.
Acetone (*10*)	1.3586/ 20°C	1.3588/ 20°C	0.7848	0.7850	56.2	56.8
n-Heptane (*1*)	1.3850	1.3851	0.6792	0.6795	98.4	98.4

Table V. Experimental Equilibrium Data

System acetone–*n*-heptane
Temperature = 65°C
Component one is ketone

x_1	y_1	π, mm	log γ_1	log γ_2	log γ_1/γ_2
0.118	0.595	581.3	0.4683	0.0153	0.4530
0.238	0.691	714.4	0.3155	0.0454	0.2702
0.413	0.768	867.5	0.2034	0.1122	0.0912
0.490	0.788	901.9	0.1565	0.1496	0.0069
0.578	0.798	954.1	0.1137	0.2332	−0.1195
0.710	0.838	999.0	0.0647	0.3184	−0.2537
0.753	0.856	1024.9	0.0590	0.3470	−0.2879
0.867	0.894	1031.0	0.0191	0.4851	−0.4660

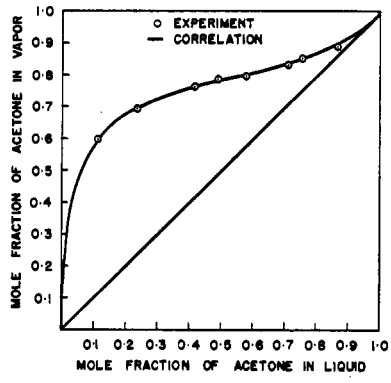

Figure 5. Vapor-liquid equilibrium of acetone–*n*-heptane mixtures at 65°C

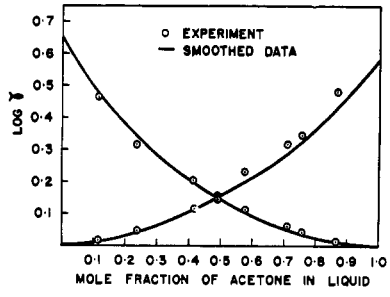

Figure 6. Activity coefficients in acetone–*n*-heptane mixtures at 65°C

NOMENCLATURE

B, C, D = constants in Redlich-Kister equations
P^0 = pure component vapor pressure, mm Hg
R = gas constant, (mm Hg) (cc)/(g-mol) (K)
T = temperature, K
V = molal volume, cc/g-mol

Greek Letters

β = second virial coefficient, cc/g-mol
γ = activity coefficient
γ^0 = terminal activity coefficient
π = total pressure, mm Hg

Subscripts

1, 2, i = component 1, 2, or i

Superscripts

L = liquid

LITERATURE CITED

(1) American Petroleum Institute, Research Project 44, "Selected values of physical and thermodynamic properties of hydrocarbons and related compounds," p 37, Carnegie Press, 1953.
(2) Barker, J. A., Brown, I., Smith, F., *Discuss. Faraday Soc.*, **15**, 142 (1953).
(3) Beare, W. G., McVicar, G. A., Ferguson, J. B., *J. Phys. Chem.*, **34**, 1310 (1930).
(4) Brown, I., Ewald, A. H., *Aust. J. Sci. Res.*, **14**, 198 (1951).
(5) Ellis, S. R., *Trans. Inst. Chem. Eng.*, **30**, 58 (1952).
(6) Ewert, M., *Bull. Soc. Chim.*, **45**, 493 (1936).

(7) Gilmont, R., Zudkevitch, D., Othmer, D. F., *Ind. Eng. Chem.*, **53**, 223 (1961).
(8) Maripuri, V. V., PhD thesis, McGill University, 1971.
(9) Perry, J. H., "Chemical Engineers Handbook," 4th ed., pp 13–15, McGraw-Hill, New York, NY, 1963.
(10) Timmerman, J., "Physico-chemical constants for pure organic compounds," pp 271–2, Elsevier, New York, NY, 1950.
(11) Wehe, H. A., Coates, J., *Amer. Inst. Chem. Eng. J.*, **1**, 241 (1955).
(12) Wohl, K., *Z. Phys. Chem. B2*, **1929**, p 77.
(13) Yvan, K. S., Ho, J. C. K., Deshpande, A. K., Lu, B. C. Y., *Chem. Eng. Data*, **8**, 549 (1963).

Received for review July 6, 1971. Accepted January 28, 1972. Work supported by the National Research Council of Canada.

Coefficient of Thermal Expansion of Pentaerythritol Tetranitrate and Hexahydro-1,3,5-trinitro-s-triazine (RDX)

HOWARD H. CADY
University of California, Los Alamos Scientific Laboratory, Los Alamos, NM 87544

Measurements have been made of the coefficients of thermal expansion as a function of temperature of single crystals of pentaerythritol tetranitrate (PETN) and hexahydro-1,3,5-trinitro-s-triazine (RDX). Two independent coefficients of linear expansion were measured for tetragonal PETN and three for orthorhombic RDX.

The thermal expansion coefficient is a second-order symmetric tensor and hence contains six independent constants for a triclinic crystal. This number is reduced for crystals with higher symmetry. Hexahydro-1,3,5-trinitro-s-triazine (RDX, $C_3H_6N_6O_6$) crystallizes with orthorhombic symmetry, and its thermal expansion is expressed by three coefficients of linear expansion measured along the principal crystallographic axes. Pentaerythritol tetranitrate (PETN, $C_5H_8N_4O_{12}$) is tetragonal, and two coefficients, one along the unique crystallographic axis and one perpendicular to it, describe the thermal expansion. The direction of measurement of the coefficient of linear thermal expansion is indicated by a subscript giving the crystal face normal to the direction of measurement—e.g., $\alpha_{(120)}$ is measured in a direction perpendicular to the (120) crystal face. It happens, for these materials, that $\alpha_{(100)}$ is measured parallel to the a crystallographic axis, and similarly $\alpha_{(010)}$ and $\alpha_{(001)}$ parallel b and c, respectively.

This paper reports measurements of the coefficients of linear thermal expansion [$\alpha = (1/L)(dL/dT)$] as a function of temperature for PETN from −160–100°C and for RDX from −160–140°C. The coefficients of volume thermal expansion [$\beta = (1/V)(dV/dT)$], as computed from the linear coefficients, are also reported.

EXPERIMENTAL

Materials. Baker Analyzed reagent-grade acetone and the chemically purest military grade PETN and RDX obtainable were used as starting materials. Nutrient stock crystals were made by recrystallization from filtered acetone solutions. Single crystals of PETN and RDX were then grown by standard cold-finger techniques from acetone solutions. The final crystals were not analyzed for chemical purity but are presumably purer than the 99 wt % purity of the starting materials. PETN and RDX are both powerful secondary explosives and should be treated with caution. The hazard of spontaneous exothermic heating to explosion and the large size of the crystals were factors determining the maximum temperatures at which expansion data were measured. The crystals were selected for measurement on the basis of optical perfection and well-developed planar faces and were rejected if they showed any evidence of nonparallel extinction with polarized light, visible distortion of an image reflected from a face, or other evidence of vicinal face development.

Apparatus. A DuPont Model 900 Thermal Analyzer equipped with a Model 941 Thermomechanical Analyzer (TMA) was used to determine linear thermal expansion. The 900 Thermal Analyzer is a solid-state electronic temperature programmer-controller which permits a wide range of temperature scanning conditions. One of several plug-in modules is the 941 TMA, which uses a movable-core differential transformer to detect vertical displacement of a sample surface as a function of temperature. The output of the transformer is specified to be linear within ±0.5% up to 0.05 in. of total displacement; however, our instrument was found to be linear to at least ±0.0625 in. from its null position. The output of the 941 module is amplified and plotted on the 900 recorder as a function of temperature on charts printed to provide direct reading of sample temperature. The maximum amplification factor for our 900 Thermal Analyzer converts a change of 0.0001232 in. of sample height to a change of 1 in. in ordinate on the chart paper.

The TMA as received from DuPont was found to be quite sensitive to changes in ambient temperature, and changes in laboratory temperature were sufficient to drive the recorder off scale when set to its maximum amplification. The amplitude of this signal was reduced to about 1 in. by moving the instrument to an air-conditioned laboratory with a constant average long-term temperature but with a short-term (15-min) temperature swing of 1°C. The Dewar cap, which is closely coupled to the differential transformer support and the top of the sample holder, was changed to provide it with constant-temperature circulating water, and the remainder of the differential-transformer support housing was isolated from rapid changes in room temperature by further insulation. These changes increased the warm-up time of the instrument to about 3 hr, but reduced the recorded ambient temperature signal to ±0.01 in.

The shape of the baseline indicated a heat leak between the sample heater and the differential transformer. Eight spaced aluminum-foil baffles were inserted inside the sample-holder tube near the Dewar cap to control radiant and convective